MASS OPTIMISATION OF VARIABLE ROTOR SPEED COMPOUND SPLIT DRIVETRAINS FOR ROTORCRAFT

Hanns Amri, hanns.amri@tuwien.ac.at, TU Wien (Austria)
Florian Donner, florian.donner@tuwien.ac.at, TU Wien (Austria)
Felix Huber, felix.huber@tuwien.ac.at, TU Wien (Austria)
Michael Weigand, michael.weigand@tuwien.ac.at; TU Wien (Austria)

July 26, 2019

Abstract

This publication is part of the international research project VARI-SPEED, which aims to enable rotor speed variation for a modern and ecologically efficient aviation. A mass estimation model for two different Sikorsky UH-60A drivetrain architectures was set up, calculating the mass of gears from the main-gearbox-input-shaft to the rotor-shaft and the tail-drive-shaft. One architecture includes a single compound split for transmission ratio variation, located close to the main rotor shaft. The other contains two compound splits, each located close to the turboshaft engines. Calculations were performed with different boundary conditions and the feasibility was analysed. The questions, if the compound split is the dominating factor of the mass optimisation and if the drivetrain architecture has an influence should be answered. The influence of design boundaries and the impact of the efficiency should be analysed. The compound split is not the dominating factor. Also the drivetrain architecture has an influence on the mass optimisation but not on the compound split configuration. Design boundaries have an impact, but the optimum is stable. The efficiency can have a higher impact than the mass. Variator engines have to be chosen according to the drivetrain architecture. Variation of the rotor speed via the gearbox enables the turboshaft engine, the rotor and the auxiliary units to operate at their optimal speeds. Rotor speed variation can overcome the divergent requirements between hover and fast forward flight, increase the efficiency and reduce noise and environmental impact of rotorcraft.

NOTATION

Symbol	Description	Symbol	Description
RPM	Revolutions per Minute	IMS	Input Module Shaft
UAV	Unmanned Aerial Vehicle	TDS	Tail Drive Shaft
FVL	future vertical lift	PDS	Pylon Drive Shaft
VTOL	Vertical Take-off and Landing	DT	Drivetrain
SFC	Specific Fuel Consumption	MTOW	Maximum Take-Off Weight
FMEA	Failure Mode Effect Analysis	BG	Bevel Gear
TSE	Turbo Shaft Engine	PG	Planetary Gear Set
MGB	Main GearBox	HG	Helical Gear Unit
IGB	Intermediate GearBox	CS	Compound Split
TGB	Tail GearBox	VA	Variator
VG	Variator Gearbox	TR	Tail Rotor
m	Mass $[kg]$	i	Transmission Ratio $[-]$
φ	Variation Range $[-]$	η	Efficiency $[-]$

Symbol	Description
NASA	National Aeronautic and Space Administration
VARTOMS	Variable rotor speed and torque matching system
CVT	Continuously variable Transmission

1 INTRODUCTION

The necessity for variable rotor speed technologies is indicated in different research and development projects in the USA, in Europe and in Russia. There are two major research programs, one is the USA "*Future Vertical Lift*" (FVL) [5] program and the second is the European Union's "*Clean Sky 2 - Fast Rotorcraft*" program [12]. The aim of both programs is to develop a high speed rotorcraft with excellent hover and vertical take-off and landing (VTOL) capabilities. In these programs the commonly used single main rotor and tail rotor configuration is not the only configuration of interest any more. New configurations, like compound rotorcraft or tiltrotor rotorcraft, are under development.

The Airbus Helicopters high speed demonstrator X^3, the previous design to the RACER, is a good example for this development. The X^3 is a compound rotorcraft with one single main rotor and two tractor propellers mounted on small wings on each side of the rotorcraft. High speed and highly efficient results could be obtained with a speed reduction of the main rotor during forward flight while additional thrust was provided by the two tractor propellers and the wings provided additional lift. The main rotors rotational speed was reduced by the variability of the turboshaft engine in fast forward flight to overcome the problem of high-speed stall on the advancing rotor blade. This setting enabled the X^3 demonstrator to achieve an unofficial level-flight speed record of $255kt$ ($472km/h$) in June 2013 [11].

The National Aeronautic and Space Administration (NASA) *Heavy Lift Rotorcraft System Investigation* [13] is a good example for the possible increase of efficiency with rotor speed variation. Three different passenger transport rotorcraft configurations were investigated. The so called *Large Civil Tiltrotor Concept*, a tiltrotor rotorcraft, was identified with the highest potential. It needs a rotor speed variation range of about 50% of the nominal RPM to be economically competitive [7].

Boeings *A160 Hummingbird* is another good example for improved rotorcraft efficiency due to rotor speed variation. The rotorcraft set up a new record in endurance flight ($18.8h$) in its class in May 2008. It was possible due to a two stage transmission gearbox for rotor speed variation [19]. Furthermore the rotor and rotor blades were designed by Karem to enable an operation at different RPM [14].

VARTOMS (Variable Rotor Speed and Torque Matching System) is an invention from Airbus Helicopters for the H145 to reduce noise, especially in urban areas, and to improve handling qualities. A speed range of 7% (from 96.5% to 103.5%) of the nominal RPM is possible [8]. A similar system is also used in the Mi-8 class helicopter and its modifications [6].

G.A. Misté presented an optimisation of variable turbo shaft engine performance with main rotor interaction of the T-700 UH-60A engine and the UH-60A main rotor in his doctoral thesis [15]. He concluded that the RPM variation has a significant impact on the specific fuel consumption (SFC) of the turboshaft engine. The main rotor RPM variation performed by the turboshaft RPM variation is less efficient than an independent optimisation of the main rotor RPM and turboshaft engine RPM.

There are three reasons for the trend to rotor speed variation as the previous examples showed. The first reason is the possibility to overcome the divergent requirements on the rotor speed in hover and in fast forward flight. This is especially interesting for the new rotorcraft configurations, like compound rotorcraft or tiltrotor rotorcraft. The second reason is the ability to reduce the emitted noise of the rotorcraft. This can increase the acceptance of rotorcraft in urban areas and in the surrounding of heliports. The third reason is the efficiency increase of the rotorcraft due to rotor speed variation which reduces the environmental impact.

An investigation of possible benefits of variable rotor speed was performed by H. Amri et. al. [2]. In a CAMRAD II simulation model of a CS-27 class helicopter a required power reduction of 23% could be achieved and different technology categories to enable rotor speed variation as well as the major risks and problems were identified.

W. Garre et. al. [10] analysed the possible efficiency increase and enhancement of the flight envelope with rotor speed variation for five different rotorcraft configuration: a single main rotor, a coaxial rotor, a coaxial compound, a tandem and a tiltrotor configuration. They could show that a rotor speed variation of up to 50% of the nominal RPM is useful for all rotorcraft configurations, but there are always some flight states where rotor speed variation is not suitable. This is at the original design region of the rotorcraft, where the reference rotor speed is equal to the optimum rotor speed.

The technology categories, defined in [2], were explored by H. Amri et. al. [4]. They found out that nowadays only two technologies are suitable for rotor speed variation: the turbine technology and the gearbox technology. An electric drivetrain is an interesting option but the components are too heavy. The turbine technology adds less additional weight but it influences the whole drivetrain and the auxiliary units. Gearbox technology is heavier but has the advantage that the RPM of different rotors can be adjusted separately and the turboshaft engine can be operated at the optimum speed as well. RPM variation with the turbine technology is suitable for a small variation range while gearbox technology is suitable for a large variation range.

W. Garre et. al. [9] analysed the rotor speed variation in the context of missions for five different rotorcraft configurations. They made a comparison between a single rotor speed, a two speed and a continuously variable transmission (CVT) variant within the missions. CVT systems showed the best benefits for utility rotorcraft. For fast rotorcraft, like compound or tiltrotor rotorcraft, the two speed transmission gains almost the same benefits as the CVT. For all configurations an efficiency increase could be identified.

P. Paschinger et. al. [17] explored three different gearbox technology groups: discrete variable gearboxes, pure CVT gearboxes and power split gearboxes. They concluded that power split gearboxes are most suitable for rotor speed variation and within this group the compound split gearboxes are the favourable solution. A functional Failure Mode Effect Analysis (FMEA) of the compound split indicated no additional risks in the drivetrain for a rotorcraft which could not be negated with additional measures.

An investigation of the kinematic behaviour and the mass of different compound split configurations was performed by H. Amri et. al. [3]. The investigation showed that the power flow in the variator path is the same for all configurations and it depends only on the spread (ratio of highest output speed to lowest output speed). The mass of the compound split configurations is different and depends on the basic transmission ratio (ratio of the input speed to the highest output speed) and the spread. They concluded that a compound split variation is most suitable when it has the lowest mass at a high basic transmission ratio in a given range of spread.

P. Paschinger et. al. [18] investigated the reliability of two different drivetrain architectures, each containing a compound split. Furthermore, they did examinations on different possible variator engines for the compound split.

So far the compound split system seems to be useful for rotor speed variation in a rotorcraft. The compound split itself was investigated according to its mass behaviour and its reliability in different design conditions. The questions which should be answered in the present paper are:

- First, if the mass of the compound split is the dominating factor for mass optimisation or if other transmission elements of the drivetrain architecture have a higher impact.
- Second, if the drivetrain architecture itself has an influence on the mass.

Furthermore, the influence of boundary conditions, like RPM restrictions or gear ratio limits, should be analysed. The impact of the efficiency of the drivetrain should be compared to the mass increase. A feasibility analysis of one optimised architecture should be carried out.

2 MODEL DESCRIPTION

The research questions should be answered for the drivetrain of the UH-60A Black Hawk, as a reference drivetrain. A detailed description of the drivetrain can be found in the UH-60A Student Handout [1]. The drivetrain consists of two turboshaft engines (TSE) which are connected to one of the input module gearboxes (IM). The input

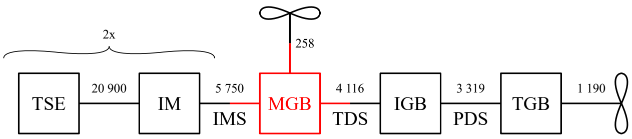

Figure 1. *Schematic of the UH-60A drivetrain*

module gearboxes are connected via a free-wheel-clutch followed by the input module shafts (IMS) to the main gearbox (MGB). The power flow is then combined in the main gearbox via a bevel gear stage with two pinion gears.

On the bevel gear wheel there is an additional bevel gear stage from which the power for the tail rotor is taken. Then the power is transferred via the tail drive shaft (TDS) to the intermediated gearbox (IGB) and then via the pylon drive shaft (PDS) to the tail gearbox (TGB) and finally to the tail rotor.

The power for the main rotor is transferred from the bevel gear wheel to the sun shaft of a planetary gear stage. The main rotor shaft is connected to the planet carrier. A schematic of the UH-60A drivetrain with the RPM of each shaft can be found in Figure 1.

The reference drivetrain has a mass of $100kg$. There the bevel gear has a gear ratio of $i_{BG} = 4.76$ and a mass of $m_{BG} = 45.2kg$. The planetary gear stage has a gear ratio of $i_{PG} = 4.68$ and a mass of $m_{BG} = 54.8kg$. These are not the original masses of the UH-60A components. The drivetrain's mass was recalculated with the load assumptions taken for the new design.

Two different drivetrain architectures for variable transmission ratio were defined for the given reference drivetrain. For each architecture the

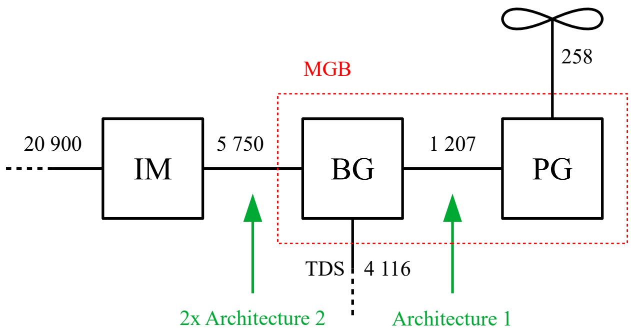

Figure 3. *Schematic of the MGB*

transmission ratio was varied for the gear stages in the main gearbox. Furthermore, all possible variants of the compound split were used in the calculation. The total transmission ratio of $i_{total} = 20.26$ was kept constant for all variations. The spread $\varphi = 1.5$ was defined according to the results in [9]. The mass was calculated for each variation point and the efficiency was calculated for each optimum. Different boundary conditions and design limitations were defined and applied to the calculation model to analyse their impact. One variation of each drivetrain architecture was selected and a design model was set up in the gearbox calculation software KISSsoft.

2.1 Drivetrain Architectures

The two architectures can be distinguished by the position of the compound split in the drivetrain, as shown in Figure 3. In architecture 1 (Figure 2) the compound split is located after the bevel gear and before the planetary gear set in the drivetrain. There are two compound splits in architecture 2. The are located before both, the bevel gear and the planetary gear set, directly on the two IMS (Figure 4).

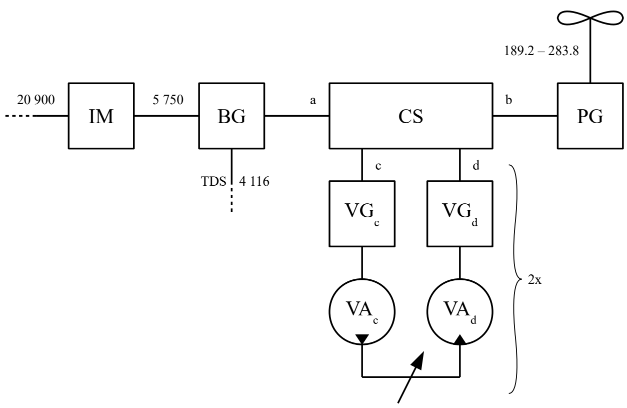

Figure 2. *Architecture 1 Model*

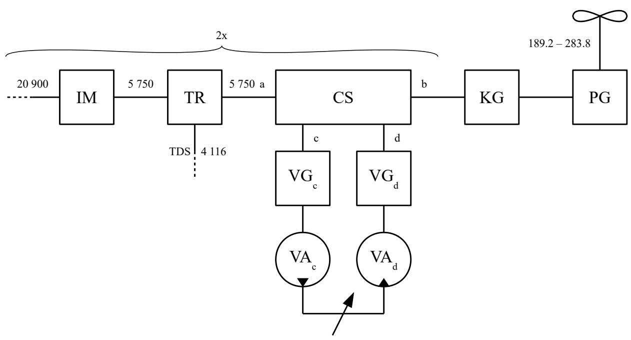

Figure 4. *Architecture 2 Model*

The tailrotor transmission in architecture 1 is connected to the bevel gear similar to the original UH-60A drivetrain. In architecture 2 a new tailrotor drivetrain has to be installed before the two compound splits to prevent the tailrotor to be affected by the variation of the rotational speed.

2.2 Compound Split and Variator

As described in [3] there are eight possible compound split configurations $A1$, $A2$, $B1$, $B2$, $C1$, $C2$, $D1$, $D2$. Their mass depends on the basic transmission ratio i_B, the spread φ and the torque. Because the compound split variants $A1$ and $A2$ as well as $B1$ and $B2$ are symmetrical, they have the same mass. Investigating the power flow of the compound split variants it turned out, that idle power occurs in variants $C2$ and $D2$. This is why this paper only analyses the masses of the four compound spit variants $A1$, $B1$, $C1$, $D1$. The compound split variants $A1$, $B1$, $D1$ are equivalent to those in [3]. However $C1$ of this paper is the same variant as $C2$ in [3]. In the following the compound split variants will be named A, B, C and D. A schematic of the variants is given in the Appendix. Also a drivetrain with a compound split e.g. A will be referred to as "drivetrain A".

The variator is a combination of a generator and a motor. The hydraulic machines that are in use are described in [18].

Because the power demand of the variator in architecture 1 exceeds the highest in [18] listed variator power, two variators were used to split the power demand. Architecture 2 also needs two variators, one for each compound split. Therefore, the number of variators are the same in architecture 1 and in architecture 2. The required power of the variators depends only on the chosen spread, which is the same for both architectures. Thus, the variator power is the same for both architectures. This means that also the mass of the variators is the same for both architectures.

The variator and the compound split are connected by a gearbox. This variator gearbox is modelled with a helical gear stage and, depending on the required transmission ratio, zero to two planetary gear sets (Figure 5).

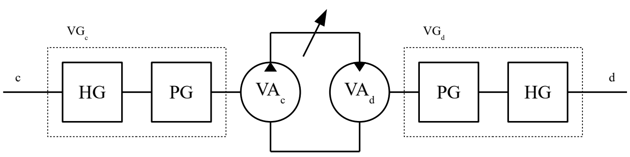

Figure 5. *Variator Gearbox*

2.3 Mass and Efficiency Estimation

The planetary gear set's mass was calculated according to the formula of [3] (Table 1).

$$
\begin{aligned}
m_{PG} &= (a_0 + a_1 \cdot i_{12} + a_2 \cdot i_{12}^2) \cdot T_1 \\
a_0 &= -0.0004038177188 \\
a_1 &= -0.0004165768445 \\
a_2 &= 0.0001785895452
\end{aligned}
$$

Table 1. *Mass function of the planetary gear set*

The compound split consists of two planetary gears with different fixed carrier gear ratios. Therefore, the compound split's mass is the sum of two planetary gear sets.

The mass of the helical gear unit is calculated using a derivation of the planetary gear set formula (Table 2). Furthermore, the assumptions was made, that a helical gear unit's mass behaves similar to the mass of a bevel gear unit. Thus, the same mass formula was used for the helical gear sets and the bevel gear sets.

$$
\begin{aligned}
m_{HG} &= m_{BG} = (b_0 + b_1 \cdot i_{SG} + b_2 \cdot i_{SG}^2) \cdot T_1 \\
b_0 &= 0.002588216233 \\
b_1 &= 0.000008547900080 \\
b_2 &= 0.0008844549095
\end{aligned}
$$

Table 2. *Mass function of the helical gear set and the bevel gear set*

The variator's mass is calculated using the formulas of [18] (Table 3) and, therefore, depends on the corner power. The corner power is the product of the maximum rotational speed times the maximum torque on each compound split variator shaft c or d (e.g. $P_{corner,c} = n_{max_c} \cdot T_{max_c}$). The variator series with the lowest mass is series 71. The total mass of two variators of that series with the given power demand is $m_{71} = 125.6kg$.

$$\text{Serie 71: } m_{71}(P_{corner}) = 0.003760 \cdot P_{corner}^{\frac{3}{2}}$$

Table 3. *Mass function of the variator series 71*

The efficiency of the planetary gear sets were calculated according to [16]. The same formulas were used for the compound splits. A fixed carrier efficiency of $\eta_{12} = 0.95$ was chosen [16]. For each architecture's optimum the efficiency of the drivetrain was calculated. The efficiency of the bevel gear, however, was neglected as a constant efficiency ratio was assumed and it affected both architectures in the same way.

2.4 Boundary Conditions

The input rotational speed $n_{in} = 5\,750 rpm$ is given. The optimal range of the main rotor speed is between +10% and −30% of the nominal main rotor speed $n_N = 258 rpm$ [10].

Therefore, the maximal rotor speed
$n_{out_{max}} = 283.8 rpm$
and minimal rotor speed
$n_{out_{min}} = 189.2 rpm$
were chosen. That leads to the drivetrain's total gear set ratio of:

$$i_{total} = \frac{n_{in}}{n_{out_{max}}} = \frac{5\,750}{283.8} = 20.26$$

This ratio is the product of the gear set ratios of the bevel gear, the planetary gear and the basic transmission ratio of the compound split.

$$i_{total} = i_{BG} \cdot i_{PG} \cdot i_B$$

As the planetary gear set ratio i_{PG} and the basic transmission ratio i_B are varied the bevel gears ratio is determined.

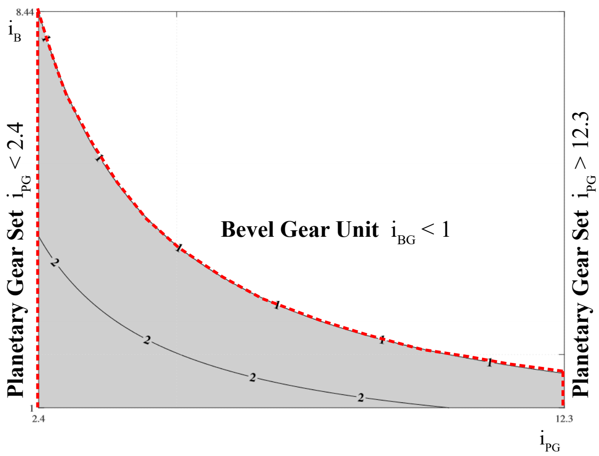

Figure 6. *Basic boundary conditions*

2.4.1 Basic Boundary Conditions

Three basic boundary conditions were chosen:

- First, the direction of rotation should not change. Thus, all gear set ratios are set as $i_j > 0$.
- Second, the rotational speed should be lowered in every stage. Therefore, all gear set ratios should be greater than or equal to 1 ($i_{BG} \geq 1, i_{PG} \geq 1, i_B \geq 1$).
- Third, the planetary gear set should be a sun-carrier transmission ($2.4 < i_{PG} < 12.3$).

The implemented boundary conditions lead to the remaining drivetrain possibilities shown in Figure 6. The grey area represents the possible gear ratio combinations for the drivetrains.

2.4.2 Design Boundary Conditions

In the next step the gear ratio boundary conditions are set for the planetary gear sets. All planetary gear sets must have a fixed carrier ratio of $-11.3 \leq i_{12} \leq -1.4$ [3]. The boundaries lead to restrictions for the basic transmission ratios of the compound splits.

2.4.3 RPM Boundary Conditions

In this case the restrictions are not caused by the gears but by the bearings. If the RPM of a shaft is too high, some bearings might be not applicable. Therefore the RPM limit is set to $6\,000 rpm$.

3 RESULTS

For both architectures separately the combined masses of the drivetrain components were analysed. Each drivetrain's architecture consists of a bevel gear, a planetary gear set and one of four compound split variants, namely *A*, *B*, *C* or *D*. The drivetrain masses are compared in each calculation point and only the drivetrain variant with the minimal mass $m_{DT_{min}}$ is shown in each point of the figures. Initially, the drivetrain was neither bound to gear ratio restrictions nor to rotational speed limits. Successively, gear ratio boundary conditions and speed limits were introduced to

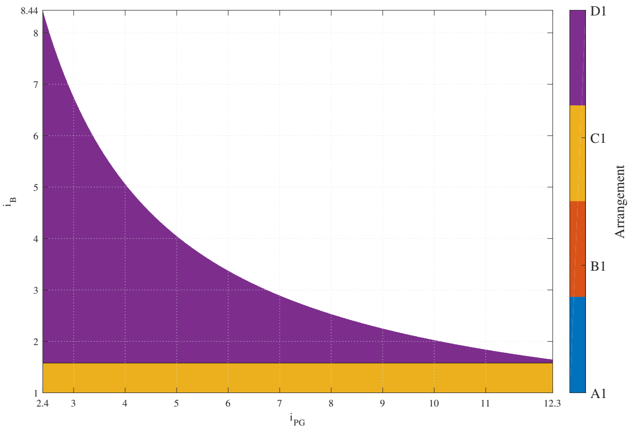

Figure 7. *Optimal drivetrain variants*

identify their influence on the mass of the drivetrain. In every step a comparison of the two architectures was made.

Furthermore, the variator path and the transmission to the TDS was analysed in terms of mass. Finally the efficiency of the drivetrain mass optima was investigated.

3.1 Mass of the Architectures

As shown in Figure 7 the mass optima are realised by the drivetrain C and D. If no gear set ratio boundaries and rotational speed limits are set the results of Figure 7 are valid for both architectures.

The minimal mass of the drivetrain of architecture 1 (Figure 8) is realised with the compound split D and has the value $m_{DT1_{Dmin}} = 59.1kg$. At this calculation point the planetary gear set's mass is $m_{PG1} = 21.8kg$ and the bevel gear unit's mass is $m_{BG1} = 21.7kg$. The compound split's mass $m_{CS1_D} = 15.6kg$ is the lowest of the components.

In the next step the lowest possible mass of the compound split D was examined. The minimal mass of the compound split D is $m_{CS1_{Dmin}} = 1.2kg$. At this calculation point the drivetrain's mass is $m_{DT1_D} = 189.3kg$. The planetary gear set is the component with the highest mass $m_{PG1} = 178.1kg$ in this drivetrain. The low gear set ratio of the bevel gear leads to it's low mass of $m_{BG1} = 10.0kg$.

Furthermore, the lowest possible mass of all compound splits was investigated. The minimum is realised by compound split C with the value $m_{CS1_{Cmin}} = 1.0kg$. The drivetrain's mass in this calculation point is $m_{DT1_C} = 228.8kg$. The mass of the planetary gear set has the value $m_{PG1} = 217.3kg$ and the bevel gear's mass is $m_{BG1} = 10.5kg$.

The minimum mass of the drivetrain with the compound split C is $m_{DT1_{Cmin}} = 84.5kg$. This value is not shown in the mass plot in Figure 8, because at this calculation point a solution of drivetrain D with a lower mass exists. The mass of drivetrain C is additional information in the plot. At this drivetrain C the planetary gear sets mass is $m_{PG1} = 31.3kg$ and the bevel gear unit's mass is $m_{BG1} = 32.5kg$. The compound split C has a mass of $m_{CS1_C} = 20.7kg$.

The drivetrain's minimal mass of architecture 2 $m_{DT2_{Dmin}} = 103.0kg$ is realised with the compound split D (Figure 9). Thus, it's minimal mass is $43.3kg$ greater than the optimum of architecture 1. The planetary gear set's mass is $m_{PG2} = 37.6kg$, the bevel gear's mass is $m_{BG2} = 61.4kg$. The mass of the sum of two compound splits is $m_{CS2_D} = 3.8kg$. Unlike in architecture 1 the minimal mass is not calculated at the minimal plan-

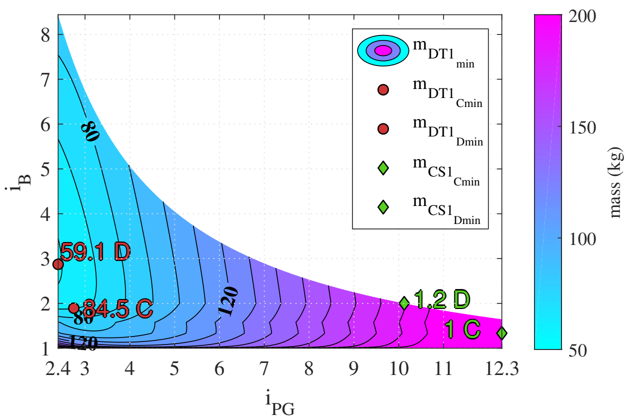

Figure 8. *Architecture 1, minimal mass plot*

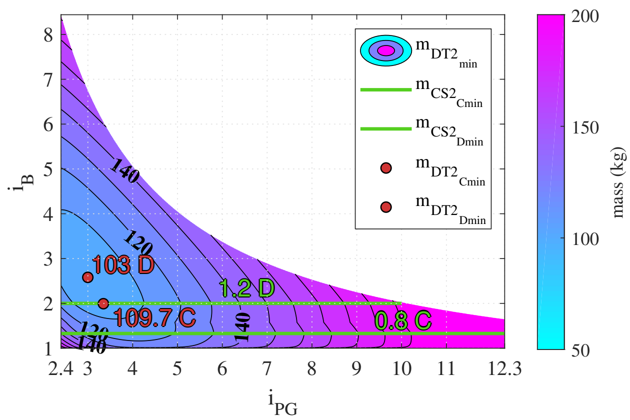

Figure 9. *Architecture 2, minimal mass plot*

etary gear ratio. While the masses of the planetary gear set and the bevel gear are bigger than in architecture 1, the the compound split's mass is comparably small.

The minimal mass of the compound split D is $m_{CS2_{Dmin}} = 1.2kg$. Due to the fact that the compound split is positioned before the bevel gear and the planetary gear set it's mass is only dependent on the basic transmission ratio. This is why the mass of the compound split is constant along constant basic transmission ratios and depicted as a line in the figures. The compound split C reaches with $m_{CS2_{Cmin}} = 0.8kg$ the lowest possible compound split mass. The minimal mass of the drivetrain C $m_{DT2_{Cmin}} = 109.7kg$ is like in architecture 1 higher than the minimal mass of the drivetrain D. The planetary gear set's mass is $m_{PG2} = 45.9kg$ and the bevel gear has the mass $m_{BG2} = 57.4kg$. The sum of the two compound splits C shows a mass of $m_{CS2_C} = 6.3kg$.

3.2 Design Boundaries

The minimal mass of architecture 1 $m_{DT1_{Dmin}} = 59.7kg$ in Figure 10 is again realised by the drivetrain D. The drivetrain's minimal mass shifts to higher basic transmission ratios, because other solutions get restricted. This leads to a small increase of the minimal drivetrain mass of $+0.6kg$. The compound split's mass increases by $+4.3kg$ and has the mass $m_{CS1_D} = 19.9kg$. The planetary gear set's mass is $m_{PG1} = 21.8kg$ and the bevel gear unit's mass has the value $m_{BG1} = 18.0kg$.

The lowest possible mass of the compound split D has under the given gear ratio boundary conditions the mass $m_{CS1_{Dmin}} = 2.8kg$. The drivetrain's mass at this calculation point is $m_{DT1_D} = 230.2kg$. While the bevel gear's mass $m_{BG1} = 10.1kg$ is relatively low the mass of the planetary gear set $m_{PG1} = 217.3kg$ is very high.

The minimal mass of compound split C $m_{CS1_{Cmin}} = 2.8kg$ is the same mass as the compound split D. Also the planetary gear set's mass in this calculation point is $m_{PG1} = 217.3kg$. Only the bevel gear's mass differs with $m_{BG1} = 11.3kg$. That leads to a drivetrain mass of $m_{DT1_C} = 231.4kg$. The optimal solution of the drivetrain C is not affected by the conditions and has a mass of $m_{DT1_{Cmin}} = 84.5kg$. The masses of all gear components remain unchanged.

The drivetrain's minimal mass of architecture 2 increases by $+2.0kg$ in Figure 11 to $m_{DT2_{Dmin}} = 105.0kg$. The planetary gear set's mass becomes $m_{PG2} = 29.2kg$ and the bevel gear's mass changes to $m_{BG2} = 61.4kg$. Also the compound split mass increases and reaches the value $m_{CS2_D} = 7.9kg$.

The minimal compound split masses also increase and have the values $m_{CS2_{Cmin}} = 2.6kg$ and $m_{CS2_{Dmin}} = 2.0kg$. Like in architecture 1 the minimal mass of the drivetrain C $m_{DT2_{Cmin}} = 109.7kg$ is not influenced by the gear ratio boundary conditions.

3.3 Rotational Speed Boundaries

Only the planets of the compound split planetary gear sets were affected by that limit and have an impact on the minimal masses.

However, in Figure 12 of architecture 1 the minimal masses of the drivetrains C and D do not

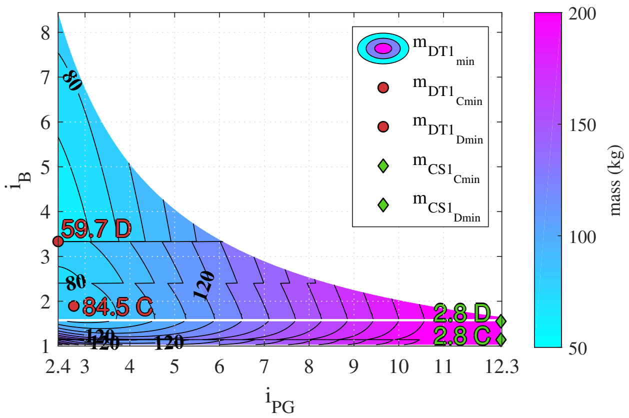

Figure 10. *Architecture 1, minimal mass plot at gear ratio boundaries*

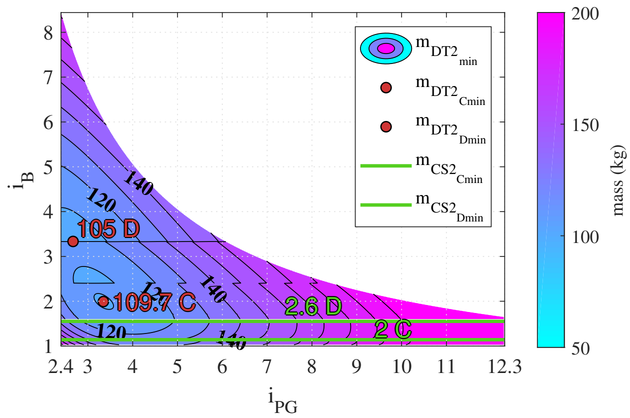

Figure 11. *Architecture 2, minimal mass plot at gear ratio boundaries*

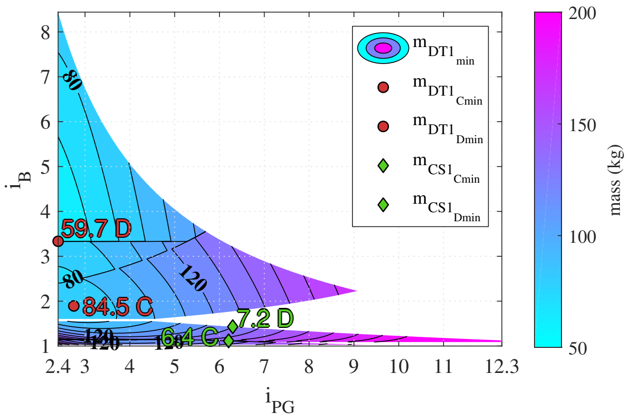

Figure 12. *Architecture 1, minimal mass plot at gear ratio boundaries and rotational speed limits*

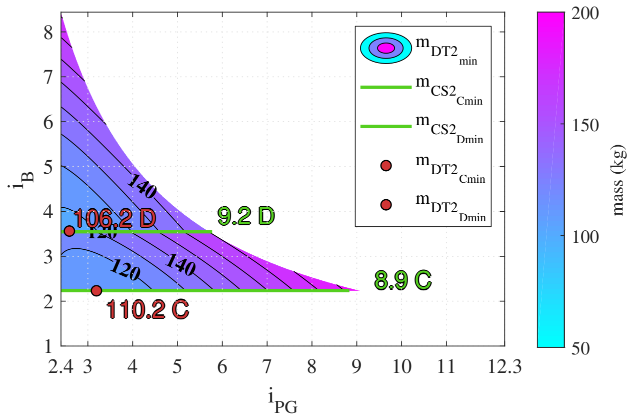

Figure 13. *Architecture 2, minimal mass plot at gear ratio boundaries and rotational speed limits*

change. Only the smallest possible compound split masses increase to $m_{CS2_{Cmin}} = 6.4kg$ and $m_{CS2_{Dmin}} = 7.2kg$.

The rotational speed limits have an influence on the solutions of architecture 2 as seen in Figure 13. Because the compound split is positioned before both, the bevel gear and the planetary gear set, the input rotational speed is $n = 5\,750rpm$ in all calculation points. Thus, various basic transmission ratios lead to high rotational speeds of planets that surpass the speed limit. Therefore, the minimal masses of the drivetrains and the compound splits increase.

The minimal mass of drivetrain in architecture 2 increases by $+1.2kg$ and has a value of $m_{DT2_{D1min}} = 106.2kg$. The planetary gear set's mass is $m_{PG2} = 27.0kg$ and the bevel gear unit shows a mass of $m_{BG2} = 70.0kg$. At this calculation point the compound split D has the mass $m_{CS2_{Dmin}} = 9.2kg$. This is also the minimal mass the compound split D can have at the chosen boundary conditions.

The mass increase of $+0.5kg$ of drivetrain C's minimum leads to the mass $m_{DT2_{C1min}} = 110.2kg$. The planetary gear set shows at this calculation point the mass $m_{PG2} = 42.3kg$ and the bevel gear unit's mass is $m_{BG2} = 59.0kg$. The compound split C has the mass $m_{CS2_{Cmin}} = 8.9kg$ which is also the lowest possible mass of the compound split C.

3.4 Minimal Drivetrain Variants

Figure 14 shows the optimal drivetrain variants of architecture 1. Boundary conditions of gear set ratios and rotational speed limits are implemented. There are solutions where the drivetrains A, C, or D have the lowest mass.

In architecture 2 (Figure 15) only the drivetrains C or D have the lowest mass.

3.5 Variator Path

Next, the variator path is taken into consideration. Whereas the mass of the variator is in every calculation point the same, the mass of the gear set, necessary to connect the variator to the compound split, changes from point to point. The variator chosen in this paper is designed for high rotational speeds and low torques. Depending on the speed and torque of the compound split shafts higher or lower gear set ratios are necessary to combine the compound split to the variator. The higher the input speed of the compound split is at

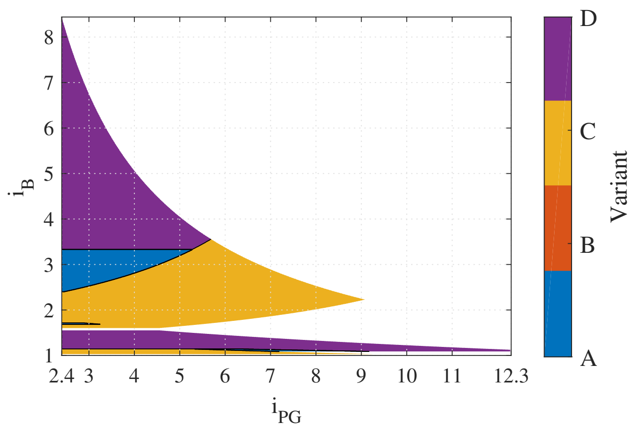

Figure 14. *Architecture 1, minimal variants at gear ratio boundaries and rotational speed limits*

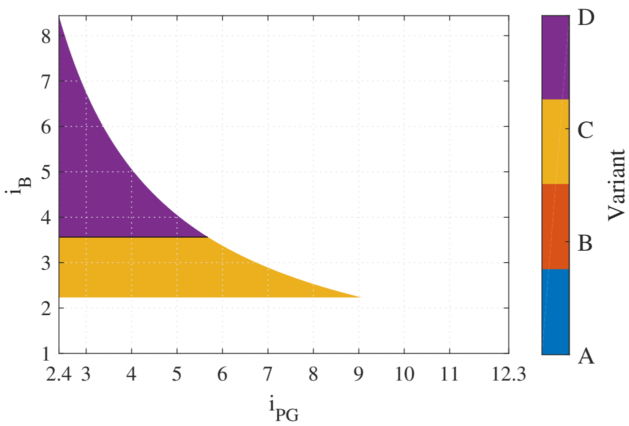

Figure 15. *Architecture 2, minimal variants at gear ratio boundaries and rotational speed limits*

a given basic transmission ratio, the higher are the rotational speeds of the compound split shafts.

At the minimal mass solution of architecture 1 the input rotational speed is low and the basic transmission ratio is high. Therefore, the gear set ratio of the variator gear is out of proportion and the mass exceeds a reasonable scale.

As architecture 2, however, has high input speeds at the compound split, lower gear ratios are needed to combine it with the variator. Thus, the gear set's mass is lower and is comparable to the mass of the components of the power path. The variator path, however, transfers only a fraction of the total power.

3.6 Transmission to Tail Drive Shaft

The mass of the bevel gear that connects the main gear box to the tail drive shaft is around $m_{TR1} = 2.5kg$ for the minimal drivetrains in architecture 1. In architecture 2 the mass model of the transmission to the tail drive shaft results in the mass $m_{TR2} = 4.1kg$. These masses are not included in the drivetrain mass optimisation.

3.7 Efficiency

The efficiency of the drivetrain mass optima was investigated in order to analyse the influence.

On the one hand, the efficiency of the compound splits was calculated. The efficiency of the two operating points was compared. The lower efficiency is at the low main rotor RPM for all configurations. In architecture 2, the masses of the optima of drivetrain C and D are similar. The efficiency of compound split C $\eta_{CS2_{Cmin}} = 96.5\%$ is higher than that of compound split D $\eta_{CS2_{Dmin}} = 94.4\%$.

On the other hand, the efficiency of the planetary gear set close to the main rotor was calculated. For architecture 1, the drivetrain was compared with and without this planetary gear set. This is possible because the compound split itself contains two planetary gears that can be used as the final stage in the drivetrain. The planetary gear set has an efficiency of $\eta_{PG_D} = 97\%$.

The efficiency increase of the drivetrain without planetary gear set had to be taken into consideration.

An estimation was made to evaluate how mass and efficiency correlate. The MTOW of $10\,000kg$ was compared to the turbine power (2 x $1\,151kW$). It was assumed that 85% of the turbine power is used by the main rotor and 15% by the tail rotor. Therefore, the 3% power loss of the planetary gear set is comparable to $255kg$ MTOW.

3.8 Design Results

One drivetrain solution in each architecture was selected and modelled in the design software KISSsoft.

For architecture 1 (Figure 16) the solution without the planetary gear set was chosen, because the positive effect of the efficiency increase weighs out the negative effects of the mass increase in terms of the overall efficiency. The KISSsoft model had a mass of $m_{DT_{D1min}} = 253.0kg$. The efficiency calculated in KISSsoft of the planetary gear set for architecture 2 is $\eta_{PG2} = 99\%$.

In architecture 2 (Figure 17) the drivetrain C was selected, because of similar masses of drivetrain C and D but better efficiency of drivetrain C. The KISSsoft model had a mass of $m_{DT_{C1min}} = 195.0kg$. The efficiency calculated in KISSsoft for the compound split for architecture 1 is $\eta_{CS1} = 98.8\%$ and for architecture 2 $\eta_{CS2} = 99.2\%$ at the lower speed.

4 DISCUSSION

To answer the research question *if the mass of the compound split is the dominating factor in the optimisation* and *if the architecture has an impact*, we need to take a closer look at the results of the mass of the architectures, given in Figure 8 and Figure 9. The drivetrain architecture 1 has a mass

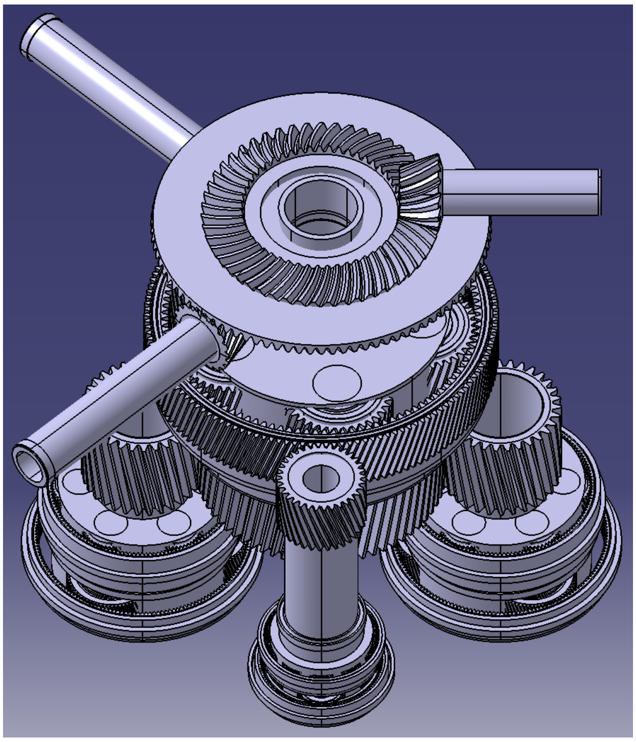

Figure 16. *Architecture 1, CAD-Model*

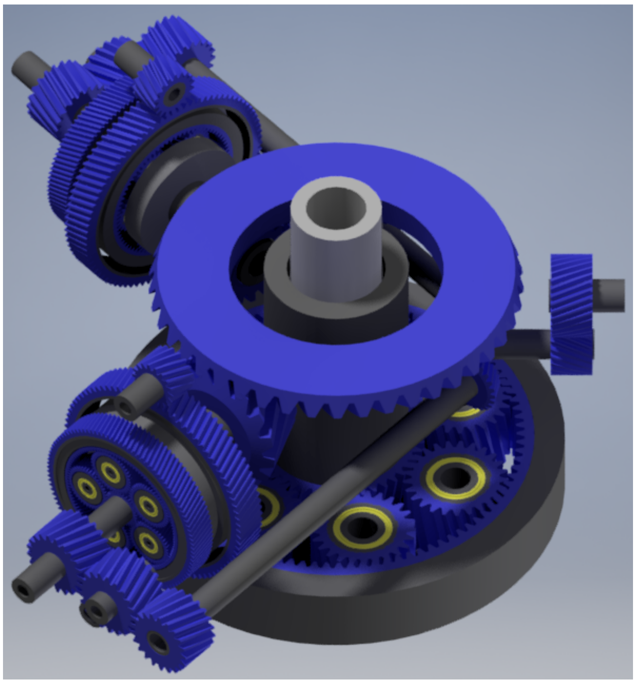

Figure 17. *Architecture 2, CAD-Model*

of $m_{DT1_{Dmin}} = 59.1kg$ and the compound split has a mass of $m_{CS1_D} = 15.6kg$, which is about 25% of the drivetrain's mass. Architecture 2 has a mass of $m_{DT2_{Dmin}} = 103.0kg$ and there the compound split has a mass of $m_{CS1_D} = 3.8kg$ which is about 4% of the drivetrain's mass. The compound split is in both architectures not the dominating factor.

Although the compound split is an additional gear stage in the drivetrain the total mass of the drivetrain architecture 1 is lower than the original one. Architecture 1 has 59% of the mass of the original drivetrain. This is possible because of the reduction of the transmission ratios of the gear stages. Especially the planetary gear set benefits from this reduction. More planets can be used in the stage and therefore the load is distributed to more gear teeth. This shows that a new design of the whole drivetrain is necessary to implement a transmission variable module (compound split). Architecture 2 has 103% in comparison to the original drivetrain.

Regarding the selection of the compound split configuration in terms of the lowest mass, it could be shown that drivetrain D is always the solution with the lowest mass of any investigated drivetrain architecture. Referring to [3], drivetrain D is the one with with the lowest mass at the highest basic transmission ratio and the given spread. Therefore, it can be concluded that the mass optimized compound split configuration is independent of the drivetrain architecture. Drivetrain architecture 1 with compound split D is the solution with the lowest mass for the chosen example.

The previously discussed results did not take the design limitations into account. It is not possible to build planetary gear sets with a fixed carrier ratio close to one and it makes no sense to build it with only two planets. Therefore, the restrictions for the fixed carrier ratio between 1.4 and 12.3 were defined and the optimisation calculation were performed with the additional limits (Figure 10 and Figure 11). Taking a look at these results show an increase of the mass of both architectures. Architecture 1 has a mass of $m_{DT1_{Dmin}} = 59.6kg$ ($+0.6kg$) and architecture 2 has a mass of $m_{DT2_{Dmin}} = 105.0kg$ ($+2.0kg$). The compound split in architecture one increases its mass by $+4.3kg$ ($19.9kg$) and in architecture 2 by $+4.1kg$ ($7.9kg$). The mass increase of the compound split is compensated by the other components. The reason for that is the increase of the basic transmission ratio of the compound split in both architectures. Therefore, the other components can reduce the transmission ratio and the mass. Consequently, there is an influence of the boundary conditions on the mass, but the mass optimum is a stable optimum, which means that small deviations have only a small impact on the result.

Next additional boundaries were applied. This has only an influence on mass optima of architecture 2. The mass of the compound split increases by $+1.3kg$ ($9.2kg$) and the architecture's mass is then $106.2kg$ ($+1.2kg$).The behaviour is similar to the design boundaries.

As the results show the drivetrain D of architecture 1 is the solution with the lowest mass. It has even less mass than the original version. This is because of the distribution of the total gear ratio onto more gear stages. However, the differences in the efficiency are not considered so far. The power losses were transferred into losses of MTOW to have a comparable value. It turned out that the architecture 1 would lead to a better helicopter performance if the last planetary gear stage would be removed. The mass of the drivetrain increases up to $111kg$, but the additional MTOW increases up to $255kg$. Therefore a net benefit of $144kg$ occurs. Drivetrains with a higher mass and a better efficiency can be preferable.

Another part which was not considered so far, is the variator path. The variator engines are the same for both architectures, but the connecting gear stages from the compound split to the variator vary in each calculation point. The model for the mass estimation of the variation path did not show feasible results. In the design there are many different possible solution to achieve lighter variator paths. What the calculation did show is, that the variator has to be chosen according to the solution of the drivetrain. In the simulation there were variator engines used which are suitable for high speeds and lower torques. They led to good results for architecture 2, because the compound split's position leads to high shaft speeds. For architecture 1 the variators did not work because all the speed reductions in the main drivetrain have to be compensated in the variator path. In the variator path there is only a small fraction of the power flow, but due to the low efficiency and the high mass of the engines it has to be designed with attention.

The design of the two architectures showed that the mass is increasing during the design compared to the calculation model. On the one hand, the mass of the planetary gear sets was underestimated. On the other hand, the efficiency losses were overestimated. Garre at al. [9] estimated a possible mass increase of about $190kg$. In this case the designed solution of architecture 2 is close to the limit. Because of the higher efficiency of the planetary gear sets architecture 1 would be a good solution too, if the planetary gear set is included. The result would have even lower weight than architecture 2.

5 CONCLUSION

- The compound split is not the dominating factor in terms of mass in the drivetrain. A new design of the whole drivetrain, including the compound split, is necessary to optimize the mass.
- The compound split configuration is independent of the drivetrain architecture. It depends on the chosen spread and is the one with the highest basic transmission ratio at its lowest mass.
- Architecture 1 with compound split D is the solution with the lowest mass.
- Design boundaries have an impact on the mass optimum of the drivetrain.
- The mass optima of the drivetrains are stable. Small deviations have only a small impact on the result.
- RPM boundaries have an impact on the mass optimum of the drivetrain and behave in the same way as design boundaries.
- The efficiency of the drivetrain and its components have a high impact on the design of the drivetrain. Even solutions with a higher mass but a better efficiency can be preferable in terms of helicopter performance.
- The properties of the variator have to be chosen carefully according to the requirements, torque and speed, based on the solution of the drivetrain.

ACKNOWLEDGEMENT

The project VARI-SPEED is supported by German Federal Ministry for Economic Affairs and

Energy in the program LuFo and by the Austrian Federal Ministry for Transport, Innovation and Technology in the program Take Off. Partners are Vienna University of Technology (Austria), Munich University of Technology (Germany) and Zoerkler Gears GmbH (Austria). The author would like to thank KISSsoft AG for the possibility to use their design software KISSsoft.

REFERENCES

[1] 110th Aviation Brigade, *UH-60A student handout - UH-60A powertrain/ rotor system 4745-3*, 74th Annual Forum Technology Display, (2008).

[2] H. Amri, R. Feil, M. Hajek, and M. Weigand, *Possibilities and difficulties for rotorcraft using variable transmission drive trains*, CEAS Aronautical Journal, 7 (2016), pp. 335–346.

[3] H. Amri, K. Hartenthaler, and M. Weigand, *Mass and kinematic analysis of compound split with simulation of the shifting process for variable rotor speed*, in 74th American Helicopter Scoiety Forum 2018, 2018.

[4] H. Amri, P. Paschinger, M. Weigand, and A. Bauernfeind, *Possible technologies for a variabel rotor speed rotorcrdaft drive train*, in 42nd European Rotorcraft Forum 2016, 2016.

[5] U. Army, *Future vertical lift (fvl) capability set 1 request for information.*

[6] M. D. Bureau, *Mi-8-helicopter flight manual*, MIL Design Bureau, 2005.

[7] J. C. W. Acree, H. Yeo, and J. D. Sinsay, *Performace Optimization of the NASA Large Civil Tiltorotr*, tech. report, NASA Ames Research Center, Moffett Field, California 94035, USA, 2008.

[8] U. D. O. Defence, *Eurocopter EC145 UH-72 Lakota Helicopter Flight Manual*, US Department Of Defence, 2008.

[9] W. Garre, H. Amri, P. Paschinger, M. Mileti, M. Hajek, and M. Weigand, *Helicopter configurations and drive train concepts for helicopter configurations and drive train concepts for optimal variable rotor-speed utilization*, in Deutscher Luft- und Raumfahrtkongress 2016, 2016.

[10] W. Garre, T. Pflumm, and M. Hajek, *Enhanced efficiency and flight envelope by variable main rotor speed for different helicopter configurations*, in 42nd European Rotorcraft Forum 2016, 2016.

[11] M. Hirschberg, *Clean sky 2 update, part 1: The airbus racer*, Vertiflite, 63 (2017), pp. 26–28.

[12] E. A. Industry, *Clean sky 2 joint technical program.*

[13] W. Johnson, G. K. Yamauchi, and M. E. Watts, *NASA Heavy Lift Rotorcraft Systems Investigation*, tech. report, NASA Ames Research Center and Langley Research Center, 2005.

[14] A. E. Karem, *Optimum Speed Rotor US Patent 6,007,298* , 1999.

[15] G. A. Misté, *Variable speed rotor helicopters: Optimization of main rotor - turbo shaft engine integration*, 2015.

[16] H. W. Mueller, *Die umlaufgetriebe - auslegung und vielseitige anwendungen*, Springer-Verlag, (1998).

[17] P. Paschinger, H. Amri, K. Hartenthaler, and M. Weigand, *Compound split drivetrains for rotorcraft*, in 43rd European Rotorcaft Forum 2017, 2017.

[18] P. Paschinger and M. Weigand, *Study on possible solutions of a compound-split transmission system for the UH-60 helicopter*, Mechanism and Machine Theory, 127 (2018), pp. 17–35.

[19] G. Putrich and C. Drawing, *FARNBOROUGH: Cutaway & technical description: Defying convention - Boeing A160 Hummingbird*, Flight Interational, 178 (2010), pp. 90–94.

APPENDIX

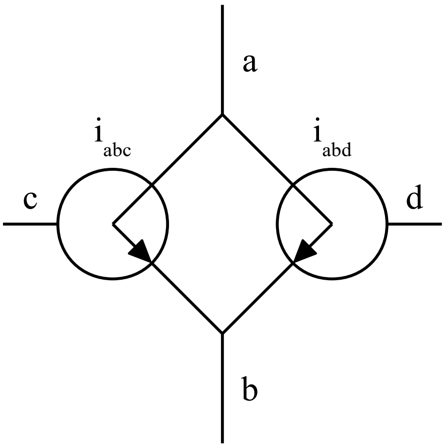

(a) *compound split variant A*

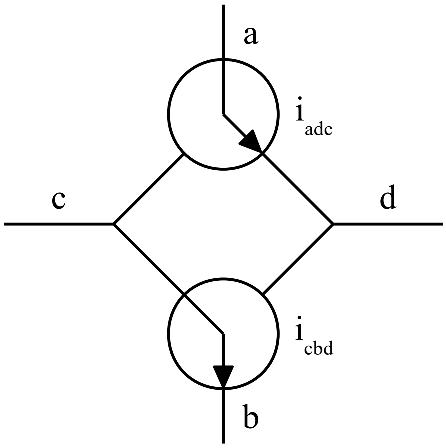

(b) *compound split variant B*

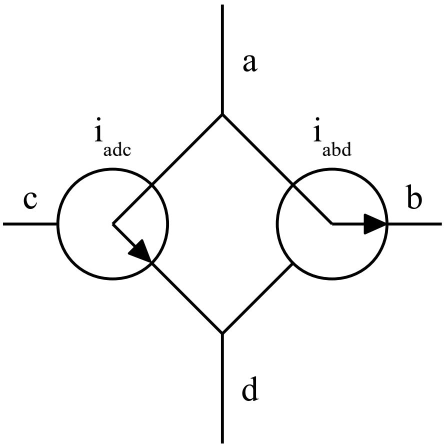

(c) *compound split variant C*

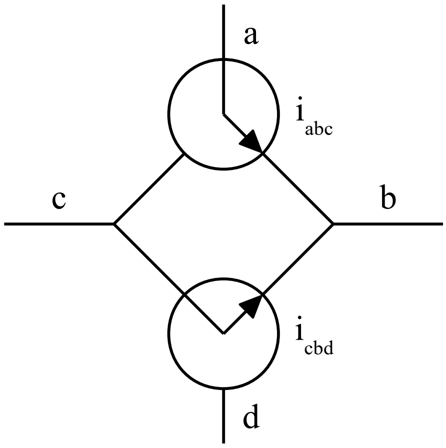

(d) *compound split variant D*

Figure 18. *graphical display of the compound split variants,*

Symbol	Description
a	input shaft of compound split
b	output shaft of compound split
c, d	shafts from compound split to variator
i_{xyz}	transmission ratio from shaft x to shaft y when shaft z is not rotating